Neuron, Vol. 17, 501–512, September, 1996, Copyright ©1996 by Cell Press

Adaptation of Ca^{2+}-Triggered Exocytosis in Presynaptic Terminals

Shyue-Fang Hsu,*‡ George J. Augustine,†‡ and Meyer B. Jackson*‡
*Department of Physiology
University of Wisconsin Medical School
Madison, Wisconsin 53706
†Department of Neurobiology
Duke University Medical School
Durham, North Carolina 27710
‡Marine Biological Laboratory
Woods Hole, Massachusetts 02543

Summary

Rapid increases in Ca^{2+} concentration, produced by photolysis of caged Ca^{2+}, triggered exocytosis in squid nerve terminals. This exocytosis was transient in nature, decaying with a time constant of approximately 30 ms. The decay could not be explained by a decline in presynaptic Ca^{2+} concentration, depletion of synaptic vesicles, or desensitization of postsynaptic receptors. Experiments in which Ca^{2+} was increased either in a series of steps or continuously at different rates suggested that the decay is caused by adaptation of the exocytotic Ca^{2+} receptor to higher levels of Ca^{2+}. This adjustable sensitivity to Ca^{2+} represents a novel property of the triggering mechanism that can be used to evaluate molecular models of exocytosis. Adaptation can limit the amount of transmitter released by a nerve terminal and permit the speed of a presynaptic Ca^{2+} rise to serve as a critical determinant of synaptic efficacy.

Introduction

Rises in Ca^{2+} concentration ($[Ca^{2+}]_i$) within presynaptic terminals cause neurotransmitter release by triggering exocytosis of synaptic vesicles (Katz, 1969). Ca^{2+}-triggered exocytosis depends on a number of distinct processes. First, Ca^{2+} must enter, diffuse, and bind to Ca^{2+}-receptor proteins subjacent to the presynaptic plasma membrane (Jahn and Südhof, 1994; Martin, 1994; Scheller, 1995; Schweizer et al., 1995). Ca^{2+}-receptor activation then causes synaptic vesicles to fuse with the plasma membrane through a complex mechanism involving an unknown number of presynaptic proteins. Although there has been much progress in identifying presynaptic proteins that could serve as Ca^{2+} receptors, the complex dynamics of Ca^{2+} in nerve terminals (Fogelson and Zucker, 1985; Simon and Llinas, 1985; Parnas et al., 1989; Adler et al., 1991) has made it difficult to establish the properties of exocytotic Ca^{2+} receptors in situ.

One way to overcome this problem is to use photolabile Ca^{2+} chelators or "caged" Ca^{2+}. Photolysis of these compounds can trigger exocytosis under more defined conditions by producing rapid and spatially uniform rises in $[Ca^{2+}]_i$ (Zucker, 1993). This approach has been widely applied to endocrine cells and has proven valuable in defining the Ca^{2+} requirements and establishing the kinetic mechanism of exocytosis in these cells (Neher and Zucker, 1993; Thomas et al., 1993; Heinemann et al., 1994). However, to date there have been only a few applications of caged Ca^{2+} in the study of neurotransmitter release from nerve terminals (Delaney and Zucker, 1990; Heidelberger et al., 1994). Here, we have used caged Ca^{2+} to characterize the presynaptic Ca^{2+} receptor in the squid giant synapse. These experiments revealed that exocytosis triggered by Ca^{2+} declines rapidly after onset. The mechanism underlying this decline appears to be adaptation of exocytosis to elevated $[Ca^{2+}]_i$ rather than depletion of releasable synaptic vesicles. Adaptation of the Ca^{2+}-sensing apparatus of exocytosis is relevant to both the molecular biology of neurotransmitter release and the physiology of synaptic transmission.

Results

The Time Course of Ca^{2+}-Triggered Exocytosis

Liberation of Ca^{2+} within nerve terminals by photolysis of the caged Ca^{2+} compound nitrophenyl-EGTA (NPE) elicited neurotransmitter release, as indicated by a rapid depolarization of the postsynaptic membrane (Figure 1A). NPE photolysis had no effect on the presynaptic membrane potential (Figure 1A). When the presynaptic $[Ca^{2+}]_i$ rise was blocked by adding 50 mM N-hydroxyethylethylenediaminetriacetic acid (HEDTA), a divalent cation chelator, to the presynaptic electrode, NPE photolysis failed to evoke an excitatory postsynaptic potential (EPSP) in more than half of approximately 20 experiments. When EPSPs could be evoked following HEDTA injection, those EPSPs were one third the amplitude of controls. In one synapse where block by HEDTA was complete, responses were subsequently obtained after continuing the injection with an NPE solution lacking HEDTA. This indicates that EPSPs evoked by illumination of NPE-filled terminals depend on the presynaptic rise in $[Ca^{2+}]_i$ and are not the result of a direct effect of light or NPE by-products.

A striking feature of the EPSP evoked by NPE photolysis was that it decayed back toward the resting potential over tens of milliseconds. The EPSP decay was a multiexponential process (Figure 1B) dominated by the fastest component with a time constant of 25.9 ± 1.6 ms (mean ± SEM; 33 synapses). A slower component of decay with a time constant of 137 ± 18 ms accounted for a smaller fraction, 21% ± 4%, of the amplitude of the EPSP (averages from 16 EPSPs in which the slow component could be clearly discerned). The EPSP shown in Figure 1 was suprathreshold, as indicated by the postsynaptic action potential. In general, EPSPs evoked by NPE photolysis had slower initial rises than action potentials evoked by electrical stimulation of the presynaptic nerve (Figure 1C). EPSPs evoked by NPE photolysis also lasted considerably longer than action potentials, decaying with a similar time course in both

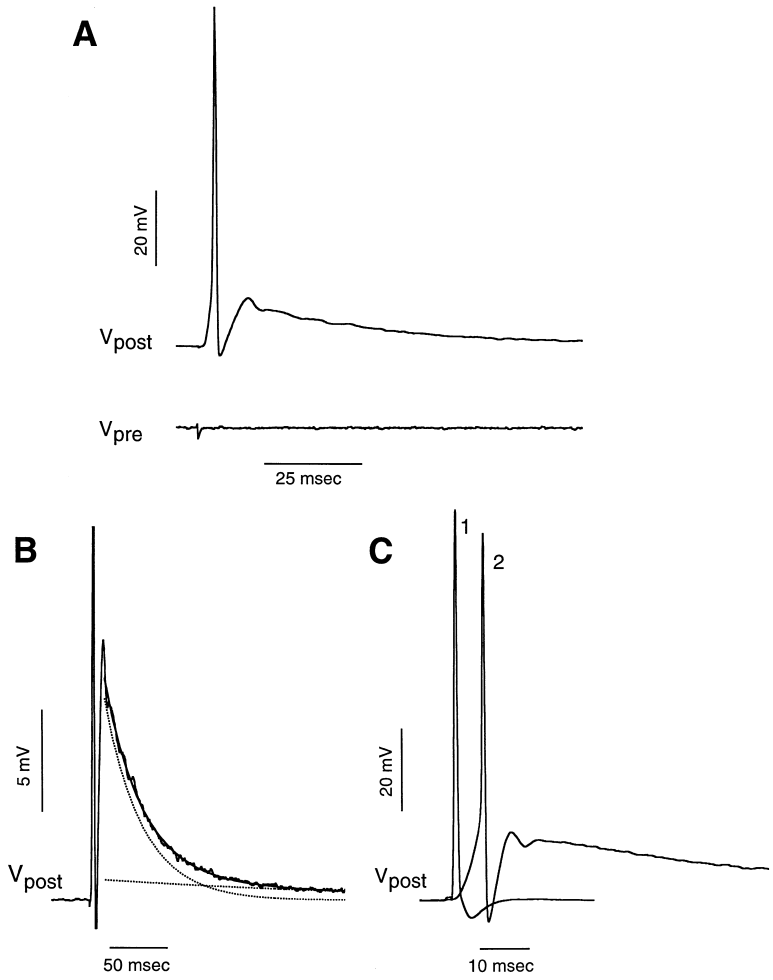

Figure 1. Responses to NPE Photolysis

(A) Simultaneous recordings of pre- and postsynaptic membrane potential. A discharge from a flash lamp photolyzed NPE within the nerve terminal. Voltage recorded in the postsynaptic cell (V_{post}) showed a suprathreshold excitatory postsynaptic response following the photolysis of NPE. Voltage recorded in the nerve terminal (V_{pre}) remained constant (except for the flash artifact, which indicates the time of the flash).

(B) V_{post} is displayed with a smaller voltage scale and longer time scale to show the shape of the EPSP evoked by NPE photolysis. The portion of the EPSP after the action potential was fitted to a sum of two exponentials. The large amplitude fast component (τ_{fast} = 33.4 ms) and small amplitude slow component (τ_{slow} = 264 ms) were drawn separately as dotted curves.

(C) A postsynaptic action potential evoked by a presynaptic action potential (1) from the same synapse is shown together with the response to NPE photolysis (2) to illustrate the slower rise and longer duration of the flash response.

sub- and suprathreshold responses. The fast components of decay had time constants of 26.2 ± 2.0 ms (29 synapses) and 23.7 ± 3.4 ms (4 synapses) for subthreshold and suprathreshold EPSPs, respectively, and these values are not significantly different ($p = 0.33$). The decay of EPSPs evoked by NPE photolysis was much slower than the membrane time constant and the gating rates of the voltage-dependent channels in the postsynaptic cell (Hodgkin, 1964). We therefore conclude that the decay reflects a decline in the postsynaptic current evoked by transmitter release and performed a series of experiments to elucidate the underlying mechanisms. In these studies, we focused our attention on the predominant fast component and restricted the analysis to subthreshold responses to avoid the complications caused by superimposed action potentials and by the nonlinear relation between transmitter release and postsynaptic potential.

EPSP Decay Is Independent of Presynaptic Ca^{2+} Concentration

Given that EPSPs are triggered by rises in presynaptic $[Ca^{2+}]_i$, we considered the possibility that a decline in $[Ca^{2+}]_i$ causes the EPSP to decay. To measure $[Ca^{2+}]_i$, we used the Ca^{2+}-sensitive fluorescent dye furaptra (Raju et al., 1989). These experiments revealed that presynaptic $[Ca^{2+}]_i$ was elevated by the photolysis of NPE, and that presynaptic $[Ca^{2+}]_i$ remained high while the EPSP decayed (Figure 2A). Complete recovery of presynaptic $[Ca^{2+}]_i$ required tens of seconds, similar to the recovery observed following Ca^{2+} entry through channels (Llinas and Nicholson, 1975; Charlton et al., 1982; Augustine et al., 1985; Swandulla et al., 1991; Smith et al., 1993). Furthermore, although larger $[Ca^{2+}]_i$ rises generated larger and faster-rising EPSPs (Figure 2A), as expected from the well-established sensitivity of transmitter release to presynaptic Ca^{2+} (Dodge and Rahamimoff, 1967; Charlton et al., 1982; Augustine and Charlton, 1986; Heidelberger et al., 1994), the time constant for decay of these EPSPs showed no significant variation with $[Ca^{2+}]_i$ up to 50 μM (Figure 2B). This indicates that the decay of the EPSP is independent of the magnitude of the presynaptic $[Ca^{2+}]_i$ rise.

Because our fluorescence measurements reflect a spatial average of $[Ca^{2+}]_i$ across the presynaptic terminal, they could fail to detect a rapid local decline in $[Ca^{2+}]_i$ that was restricted to a small region around active zones, the microscopic sites of exocytosis. For example, if a very powerful Ca^{2+} transport system were highly concentrated around active zones, it could act as a Ca^{2+} sink to create "holes," or domains of low $[Ca^{2+}]_i$, much as Ca^{2+} channels have been proposed to create domains

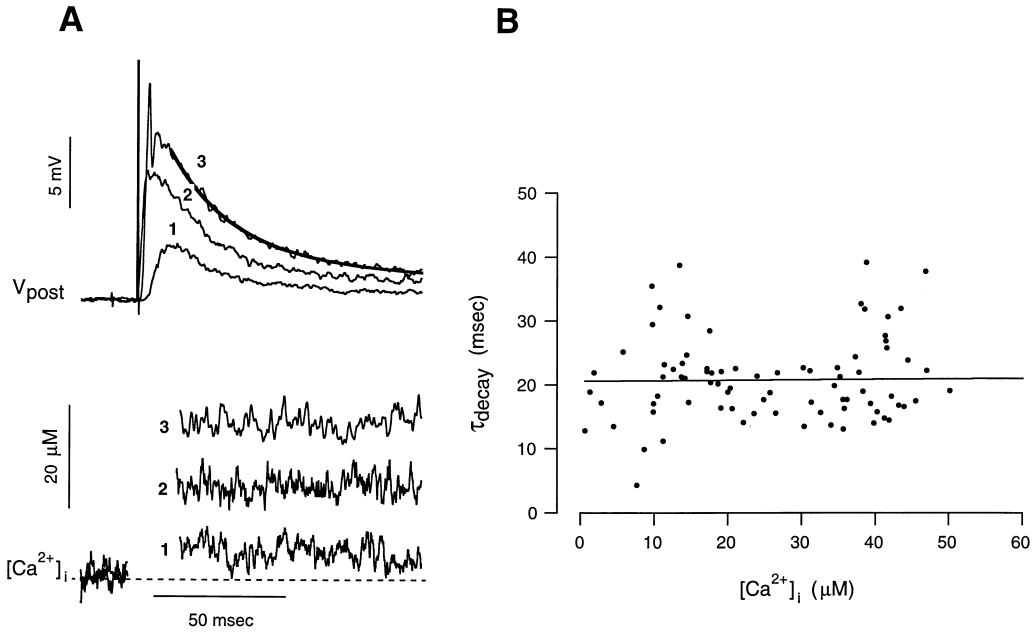

Figure 2. Rises in $[Ca^{2+}]_i$ during NPE Photolysis

(A) Flash lamp discharges of three different intensities were used to produce $[Ca^{2+}]_i$ steps and EPSPs of three different sizes. During the decay of the EPSPs, $[Ca^{2+}]_i$ remained essentially constant (dashed line shows the zero $[Ca^{2+}]_i$ level here and in other figures below). The best-fitting sum of two exponentials is drawn through the largest EPSP (τ_{fast} = 24.5 ms; τ_{slow} = 180 ms).

(B) A plot of the fast time constant of EPSP decay versus $[Ca^{2+}]_i$ showed no significant correlation ($R = 0.018$, $p > 0.50$ for 83 points, 9 synapses), indicating that the EPSP decay is independent of $[Ca^{2+}]_i$.

of high $[Ca^{2+}]_i$ (Fogelson and Zucker, 1985; Simon and Llinas, 1985; Parnas et al., 1989; Adler et al., 1991; Schweizer et al., 1995). To address this possibility, we added 50 mM HEDTA (a Ca^{2+} chelator with an effective K_d of 3 μM) to the solution injected into the nerve terminal. This mobile buffer will enhance Ca^{2+} diffusion within the nerve terminal and provide a reservoir of Ca^{2+} for release into newly created domains of low $[Ca^{2+}]$. In this way, HEDTA should reduce any spatial gradients caused by active removal. As noted above, in a majority of the experiments with HEDTA injection into the presynaptic nerve, EPSPs could not be evoked by NPE photolysis. In a few HEDTA-injected synapses, EPSPs could be evoked, but the mean amplitude was reduced from the control value of 8.3 ± 1.1 mV (29 synapses) to 2.7 ± 0.5 mV (6 synapses, $p = 0.0015$). These results indicate that HEDTA was having the expected buffering effect on $[Ca^{2+}]_i$. However, as shown in Figure 3A, small EPSPs evoked in the presence of HEDTA still decayed with similar kinetics (τ = 22.7 ± 2.0 ms; 6 synapses; $p = 0.22$ compared to control). If active removal were selectively depleting Ca^{2+} from small regions around active zones, HEDTA should counteract this effect. The similar rate of decay obtained with HEDTA thus suggests that local removal of Ca^{2+} is unlikely and that the decay of exocytosis cannot be explained by a highly concentrated Ca^{2+} active transport system near active zones of transmitter release.

Although $[Ca^{2+}]_i$ appears constant during the decay of the EPSP, it is possible that $[Ca^{2+}]_i$ is much higher immediately after photolysis, but decays rapidly to the level observed before furaptra fluorescence can be measured. Transient rises in $[Ca^{2+}]$, or Ca^{2+} spikes, occur when Ca^{2+} is liberated very rapidly and subsequently binds either to unphotolyzed free chelator (Zucker, 1993; Ellis-Davies et al., 1996) or endogenous Ca^{2+}-binding proteins (Neher and Augustine, 1992). Ca^{2+} spikes lasting a few hundred microseconds were reported after photolysis of NPE by a 35 ns laser pulse (Ellis-Davies et al., 1996). Thus, although the results in Figure 2 indicate that the decay of exocytosis is not a simple reflection of a decay in $[Ca^{2+}]_i$, the possibility remains that $[Ca^{2+}]_i$ decays more rapidly than can be measured and that the decay of the EPSP reflects a slower process such as the rate of dissociation of Ca^{2+} from a receptor that triggers exocytosis. We therefore attempted to determine the relevance of Ca^{2+} spikes to the decay of transmitter release.

A theoretical analysis of NPE binding kinetics can be used to estimate the expected duration of spikes arising from Ca^{2+} binding to unphotolyzed NPE. The relevant association process is

$$Ca + NPE \underset{\beta}{\overset{\alpha}{\rightleftarrows}} Ca\text{–}NPE$$

with a forward rate, α, and a reverse rate, β. If we neglect the effects of endogenous Ca^{2+}-binding proteins, then after a spike $[Ca^{2+}]$ will approach equilibrium with the following time course (Moore, 1972).

$$[Ca^{2+}] = [Ca^{2+}]_t - \frac{be^{(\alpha t + K)(a-b)} - a}{e^{(\alpha t + K)(a-b)} - 1} \quad (1)$$

where $[Ca^{2+}]_t$ is the sum of the concentrations of bound and free Ca^{2+} and the integration constant K was adjusted to give the initial value for free $[Ca^{2+}]$. a and b are defined as

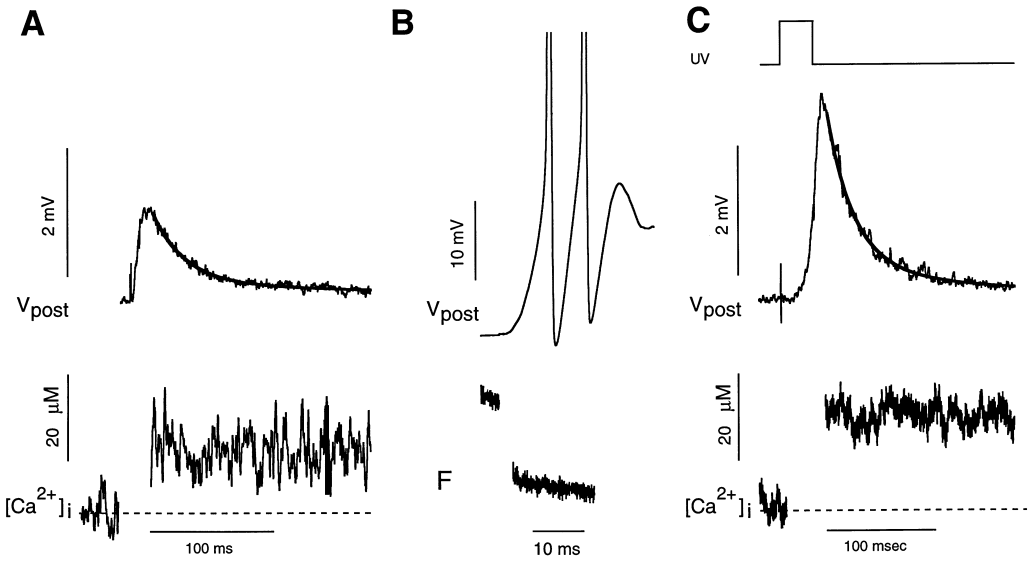

Figure 3. Simultaneous Recordings of Postsynaptic Potential and Presynaptic $[Ca^{2+}]_i$

(A) In a nerve terminal injected with NPE together with the chelator HEDTA (50 mM added to the presynaptic electrode filling solution), photolysis of NPE with a flash lamp discharge produced smaller $[Ca^{2+}]_i$ rises and smaller EPSPs. These EPSPs decayed with kinetics similar to controls performed with NPE alone (see text). For the fit shown, $\tau_{fast} = 26.1$ ms and $\tau_{slow} = 190$ ms.

(B) Furaptra fluorescence and postsynaptic potential on an expanded time scale show that $[Ca^{2+}]_i$ is constant 2 ms after the end of photolysis. A $[Ca^{2+}]_i$ increase of 17 μM (computed from equation 2) was produced by a 1 ms pulse of high intensity light from the modulated light source described in Experimental Procedures. Low intensity light from the same source provided the excitation light for the furaptra signal, but also caused weak uncaging as indicated by the slight downward slope in fluorescence. The postsynaptic response was especially strong in this experiment, firing two action potentials in rapid succession. Note that fluorescence rather than $[Ca^{2+}]_i$ is shown to emphasize the rapid equilibration after photolysis.

(C) Continuous illumination with an arc lamp for 30 ms photolyzed NPE to produce an EPSP. The time of UV illumination is indicated schematically above. Both here and in other figures below, the actual time of illumination was approximately 5 ms later than indicated due to the delayed response of the shutter. The best-fitting sum of two exponentials is drawn through the EPSP ($\tau_{fast} = 24.2$ ms; $\tau_{slow} = 119$ ms).

$$a = {}^1/_2\left[[N]_t + [Ca]_t + K_d + \sqrt{([N]_t + [Ca]_t + K_d)^2 - 4[N]_t[Ca]_t}\right]$$

and

$$b = {}^1/_2\left[[N]_t + [Ca]_t + K_d - \sqrt{([N]_t + [Ca]_t + K_d)^2 - 4[N]_t[Ca]_t}\right]$$

where $[N]_t$ is the sum of the concentrations of bound and free NPE, and K_d is the dissociation constant (β/α). Equation 1 can be used to estimate a theoretical upper limit to the duration of a Ca^{2+} spike in our experiments. If initial $[N]_t$ is at the low end of our estimated range (0.2 mM; see Experimental Procedures), is 67% loaded, and 50% photolyzed, $[Ca^{2+}]_i$ will first rise to 66 μM prior to reassociation, and then decline to 34 μM after equilibrating with the remaining NPE. Using values for α and β from Ellis-Davies et al. (1996), equation 1 indicates that the time required for 50% equilibration is 0.7 ms. Assuming higher $[N]_t$ or considering the effects of Ca^{2+}-binding proteins will make the spike decay faster. The higher ionic strength and viscosity of squid cytoplasm could slow the association rate and make a spike last as much as 3-fold longer to give a maximum duration of 2 ms.

To see whether Ca^{2+} spikes are present in our experiments, we attempted to resume $[Ca^{2+}]_i$ measurement as early as possible after photolysis. Using light from a modulated arc lamp (see Experimental Procedures), we switched between low and high intensity illumination while monitoring furaptra fluorescence. A 1 ms pulse of high intensity light photolyzed NPE and produced a large EPSP. Returning to low intensity light enabled us to measure $[Ca^{2+}]_i$ as soon as the light source switching was complete (Figure 3B). This experiment failed to reveal a Ca^{2+} spike in three synapses, indicating that if a Ca^{2+} spike occurs, then it lasts less than 2 ms. This result, along with the theoretical arguments above, suggests that if Ca^{2+} spikes are present in our experiments, then they last less than 2 ms.

We can use the knowledge that Ca^{2+} binding processes equilibrate in less than 2 ms to design an experiment to raise $[Ca^{2+}]_i$ without producing a spike. Ca^{2+} spikes occur when Ca^{2+} is liberated more rapidly than it is subsequently bound. If Ca^{2+} is liberated more slowly, Ca^{2+} and Ca^{2+}-binding molecules will remain close to equilibrium, and spikes will not occur. Since both theoretical and experimental evidence discussed above indicates that the relevant binding processes require less than 2 ms, we slowed the rate of photolysis by using 20-fold weaker illumination from a continuous light source (75 W Xe, see Experimental Procedures). This allowed us to produce $[Ca^{2+}]_i$ rises comparable in size to those produced by the flash lamp, but spread out over a period of 30 ms. These slower $[Ca^{2+}]_i$ rises still elicited EPSPs (Figure 3C), and these EPSPs decayed with the same rate as the EPSPs evoked by more rapid $[Ca^{2+}]_i$ rises ($\tau = 28.9 \pm 3.2$ ms; 12 synapses; $p = 0.24$ compared with $\tau = 26.2 \pm 2.0$ ms for EPSPs evoked by flash lamp discharges). Reducing the rate of photolysis

an additional 3.1-fold by placing a neutral density filter in the path of the continuous light source still resulted in large EPSPs, which decayed with similar kinetics (τ = 28.4 ± 1.6 ms; 11 synapses; p = 0.26). Thus, with photolysis over time intervals far longer than the theoretical and experimental estimates of the time required for Ca^{2+} reassociation, we still saw EPSPs with the same transient behavior. These results thus suggest that Ca^{2+} spikes are not essential either for triggering release or for the subsequent decay.

Previous work in the squid synapse with another caged Ca^{2+} compound, DM-nitrophen, showed transient EPSPs qualitatively similar to those shown here (Delaney and Zucker, 1990). In contrast with NPE, which binds Mg^{2+} poorly (Ellis-Davies and Kaplan, 1994), DM-nitrophen interacts with Mg^{2+} to increase the tendency of this form of caged Ca^{2+} to produce Ca^{2+} spikes (Zucker, 1993). To see whether Ca^{2+} spikes can influence the decay of EPSPs, we performed experiments with DM-nitrophen. As shown previously in this synapse (Delaney and Zucker, 1990), photolysis of DM-nitrophen produced $[Ca^{2+}]_i$ rises that partially recovered in 10–30 ms (four experiments; data not shown). The EPSPs elicited by DM-nitrophen photolysis decayed more rapidly than those elicited by NPE photolysis (τ = 15.2 ± 3.1 ms; p = 0.03 compared with τ for NPE), suggesting that Ca^{2+} spikes can accelerate the decay of EPSPs. If NPE also produced a Ca^{2+} spike, it would have to be faster than the spike produced DM-nitrophen to avoid detection. However, if such a spike were relevant to the decay, then EPSPs elicited by NPE photolysis should decay more rapidly than EPSPs elicited by DM-nitrophen photolysis. This is the opposite of what was seen, so the results obtained with DM-nitrophen provide additional evidence against Ca^{2+} spikes influencing the decay of EPSPs produced by NPE photolysis.

Additional tests of the relevance of Ca^{2+} spikes were provided by experiments employing a series of 25 ms exposures from a continuous light source to raise $[Ca^{2+}]_i$ in a sequence of five steps (Figure 4). The first step in $[Ca^{2+}]_i$ was very small, and the resulting EPSP was insignificant. However, each of the four subsequent exposures produced larger rises in $[Ca^{2+}]_i$ that were accompanied by transient EPSPs. The first exposure photolyzed the most NPE and therefore should have liberated the largest amount of Ca^{2+}. The small rise in $[Ca^{2+}]_i$ at this point means that the liberated Ca^{2+} was sequestered by unphotolyzed NPE and Ca^{2+}-binding proteins. Thus, the failure of the first exposure to produce an EPSP means either that slower photolysis failed to produce a Ca^{2+} spike (as argued above), or that transient $[Ca^{2+}]_i$ rises failed to elicit secretion (Neher and Zucker, 1993). Either interpretation supports the position that the decay of EPSPs is not due to Ca^{2+} spikes.

A second point from Figure 4 relevant to Ca^{2+} spikes is that each EPSP in the series showed a large decay with similar kinetics. The time constants were 28.9 ± 3.2, 23.4 ± 3.1, and 25.9 ± 4.0 ms (12 synapses) for the decay of EPSPs evoked by the second, third, and fourth exposures, respectively, and these values were not significantly different. At equilibrium $[N]_{bound}/[NPE]_{free} = [Ca^{2+}]_i/K_d$, and with K_d = 80 nM (Ellis-Davies et al., 1996; this value could be two or three times higher in squid

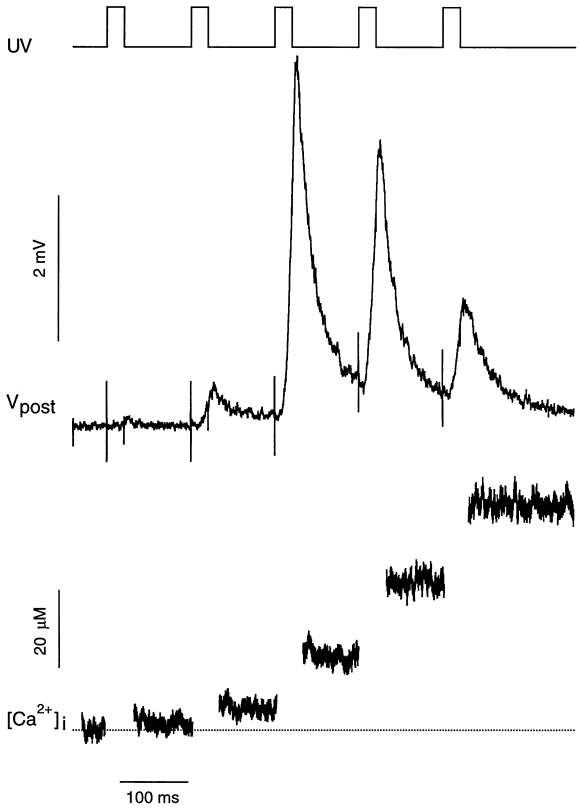

Figure 4. Response to Multiple Exposures

Five successive 25 ms exposures to light from an arc lamp, applied at 100 ms intervals, evoked a series of EPSPs and rises in presynaptic $[Ca^{2+}]_i$ (UV illumination indicated schematically above). Each exposure that increased $[Ca^{2+}]_i$ evoked a transient EPSP. The first exposure produced only a small rise in $[Ca^{2+}]_i$ and a small EPSP. The time constants for the decays of the responses to the second, third, and fourth exposures were indistinguishable (see text).

cytoplasm), free NPE will be very low once $[Ca^{2+}]_i$ rises above a few micromolar. Association of Ca^{2+} with free NPE therefore cannot cause spikes after the second exposure, indicating that spikes arising in this way cannot explain the decay of those EPSPs. Although dissociation constants of endogenous Ca^{2+} buffers are not available, if rebinding of Ca^{2+} by endogenous buffers played a role in the decay, then this effect would also be reduced in the later EPSPs of Figure 4 as these buffers became saturated, but no evidence for this was seen.

In conclusion, these experiments indicate that changes in $[Ca^{2+}]_i$ play little if any role in the decay of EPSPs evoked by NPE photolysis. The spatial average of $[Ca^{2+}]_i$ remained constant while the decay was in progress, and various tests failed to reveal influences arising from spatial or temporal anomalies in $[Ca^{2+}]_i$.

EPSP Decay Is Not Caused by Vesicle Depletion

A second possible mechanism for the decay of EPSPs elicited by release of caged Ca^{2+} is vesicle depletion. Other types of secretory cells produce transient exocytosis in response to sustained elevations in $[Ca^{2+}]_i$, and this usually is attributed to depletion of a pool of

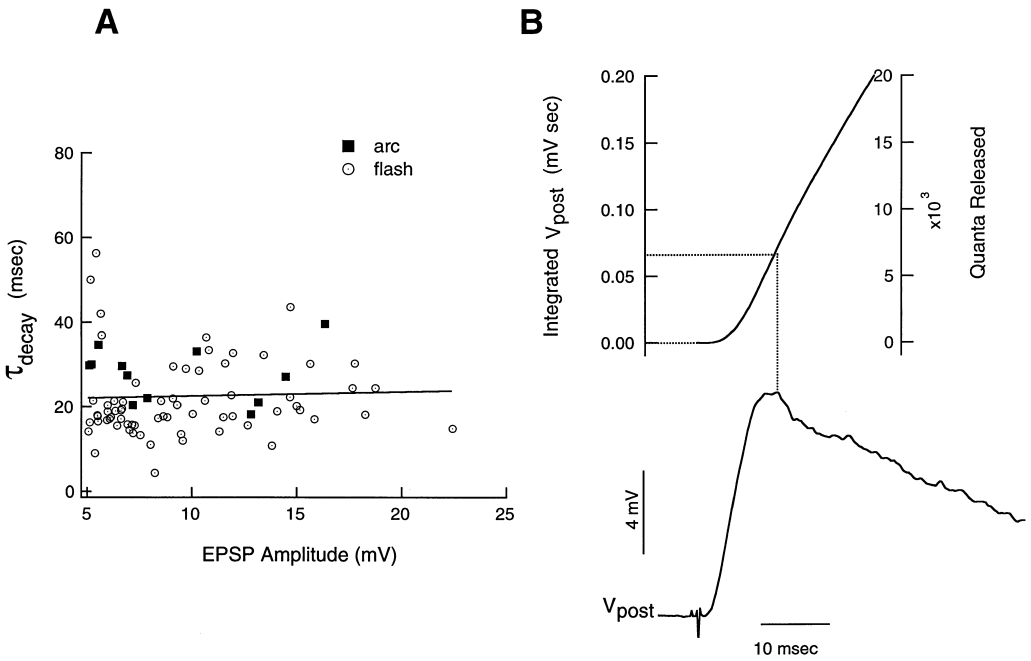

Figure 5. Absence of Vesicle Depletion during the EPSP Decay

(A) Plot of time constant for EPSP decay versus the amplitude of the EPSP. Linear regression analysis (line shown) indicated no significant correlation ($R = 0.09$; $p > 0.2$; 80 points from 35 synapses).

(B) An integrated EPSP showed the amount of release that occurred prior to the onset of decay. A dotted line was drawn up from the peak of the EPSP to its integral, and then left to the y-axis to indicate the extent of release at that point in time. The integral of the EPSP shown was 0.07 mV•s at the peak, corresponding to the release of approximately 7000 quanta (see text for explanation and average value).

primed vesicles that are available for immediate release (Neher and Zucker, 1993; Thomas et al., 1993; Heidelberger et al., 1994; Heinemann et al., 1994). We therefore performed experiments to evaluate the possible contribution of vesicle depletion to the decay of EPSPs.

The response shown above to a series of steps in $[Ca^{2+}]_i$ (Figure 4) is relevant to the depletion hypothesis. Light was applied at intervals timed to produce a new $[Ca^{2+}]_i$ rise during the decay of the preceding EPSP. The triggering of more exocytosis during the decay of the previous EPSP indicates that vesicles are available during the decay. The results shown in Figure 4 (along with five other experiments) were obtained with small synapses that fit within the field of view to allow illumination of the entire nerve terminal. Regardless of how much of the synapse was illuminated, the results were the same, indicating that the early and later responses in Figure 4 are not likely to arise from different regions of the synapse receiving illumination of different strength. The repeated responses shown in Figure 4 thus demonstrate that primed vesicles were not depleted but remained available for exocytosis while an EPSP decayed. However, depletion may explain the decline in peak amplitude observed after the third response of the series shown in Figure 4, and this would suggest that more than one light-evoked EPSP is needed to cause depletion.

Depletion of vesicles at synapses increases in proportion to the amount of transmitter released (Kusano and Landau, 1975), so that if depletion is responsible for the decay, EPSPs with greater amplitudes should decay more rapidly. However, Figure 2A above showed that EPSPs with different amplitudes decayed with similar kinetics. A plot of τ versus EPSP amplitude confirmed this observation; there was no significant correlation between these two quantities (Figure 5A). Thus, EPSPs caused by exocytosis of smaller or larger numbers of vesicles decayed with the same rate, in contrast with what would be expected if the decay were caused by vesicle depletion.

A presynaptic action potential evokes the release of approximately 50,000 quanta (Llinas et al., 1982; Augustine and Eckert, 1984) without causing significant quantal depletion (Kusano and Landau, 1975). If release induced by photolysis of NPE were depleting synaptic vesicles, an even greater number of quanta would have to be released. We can estimate the number of quanta released in our experiments by integrating the EPSP elicited by NPE photolysis and dividing this integral by the integral estimated for a single quantum (Delaney and Zucker, 1990). The integrated EPSP produced by NPE photolysis was 0.040 ± 0.006 mV•s (26 synapses) at the time when the decay began (Figure 5B). With the integral of one quantum estimated as 10^{-5} mV•s (Augustine and Eckert, 1984), we calculate that the decay begins after 4000 ± 600 quanta have been released. This should constitute only a small fraction of the vesicles released by an action potential, and thus is only a small fraction of the primed vesicles available for release in the nerve terminal. Consideration of the fraction of the synapse illuminated may reduce this excess by a factor that we estimate to be less than two. But when one considers the fact that weaker flashes of light produced

smaller EPSPs (Figure 2A), and these smaller EPSPs begin to decay at about the same time and with the same rate (Figure 2B), then it would appear that the decay can commence after release of an even smaller number of vesicles. Alternatively, with approximately 10,000 to 20,000 active zones in a synapse (Pumplin et al., 1981), the release of 4000 quanta corresponds to one vesicle per 2.5 to 5 active zones, further suggesting an excess of vesicles. These comparisons indicate that the amount of release prior to the onset of decay is far less than both the number of quanta released by a single presynaptic action potential and the number of available vesicles estimated to be present in this synapse.

Finally, we tested the depletion hypothesis by using physiological stimuli to elicit Ca^{2+} entry through Ca^{2+} channels. Presynaptic action potentials were used to evoke transmitter release during the decay of an EPSP produced by NPE photolysis. Three out of ten such experiments were performed with illumination of nearly the entire nerve terminal, in which electrically evoked release from regions that escaped illumination is unlikely. If the decay of EPSPs evoked by NPE photolysis were due to vesicle depletion, then electrically evoked EPSPs should be reduced in proportion to the extent of decay. In contrast, we found that EPSPs evoked by presynaptic action potentials at various times after NPE photolysis were slightly enhanced relative to controls (Figures 6A and 6B). This enhancement has been reported previously using DM-nitrophen (Delaney and Zucker, 1990) and probably reflects a modest facilitation of synaptic transmission by Ca^{2+} (Katz and Miledi, 1968; Charlton et al., 1982; Swandulla et al., 1991). Taken together, the results in Figures 4–6 argue against depletion of vesicles as a mechanism for the decay of EPSPs elicited by caged Ca^{2+}.

Further, these results also indicate that postsynaptic desensitization does not play a role in the decay. It has been shown that the glutamate receptors in this synapse are desensitized by neurotransmitter (Kelly and Gage, 1969), but the time constant for desensitization is on the order of one second (Corrie et al., 1993), and therefore much too slow. Moreover, the results shown in Figures 4 and 6 are inconsistent with the finding that once receptors are desensitized they cannot be activated by further increases in neurotransmitter concentration (Corrie et al., 1993). It is also unlikely that each response reflects the activation and desensitization of different groups of receptors. We estimated above that one out of 2.5 to 5 active zones had released a vesicle by the onset of the decay, but by the time of the next $[Ca^{2+}]_i$ step or presynaptic action potential, the integral of the EPSP had increased by at least 5-fold, so that all of the active zones had released vesicles. This point and the much slower rate of desensitization (Corrie et al., 1993) make it unlikely that each response reflects the activation and desensitization of spatially distinct sets of receptors. It should be noted that any mechanism of decay with a postsynaptic locus would necessarily require release of transmitter to be sustained following the photolysis of NPE. Since sustained release would desensitize receptors and prevent subsequent responses such as those shown in Figures 4 and 6, we can conclude that the decay in synaptic transmission occurs at a step upstream from postsynaptic receptor activation.

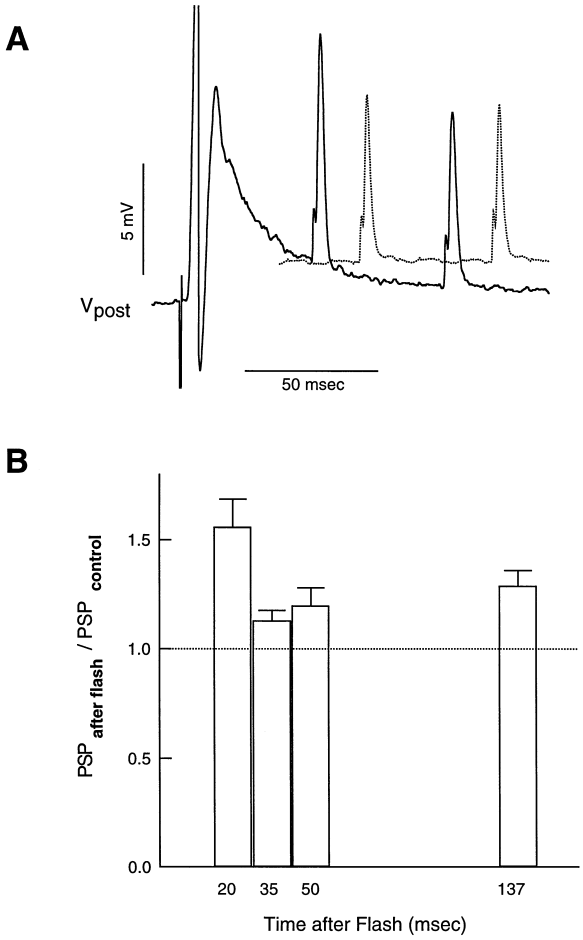

Figure 6. Synaptic Transmission after the EPSP Decay

(A) Electrical stimulation of the presynaptic terminal evoked EPSPs 50 and 100 ms after NPE photolysis. The two electrical responses evoked after NPE photolysis were larger than control electrical responses (dashed trace offset to facilitate comparison) evoked in the absence of NPE photolysis.

(B) Peak amplitudes of EPSPs evoked by electrical stimulation at various times after NPE photolysis (as in [A]) were divided by the amplitudes of the corresponding control EPSPs, evoked prior to NPE photolysis, and plotted versus time interval between photolysis and electrical stimulation.

Adaptation and the Sensitivity of EPSPs to the Rate of Rise of $[Ca^{2+}]_i$

Because our experiments ruled out decreases in $[Ca^{2+}]_i$, depletion of vesicles, presynaptic voltage changes, and postsynaptic receptor desensitization, some other mechanism must account for the decay of EPSPs evoked by NPE photolysis. We therefore considered the possibility that the decay of these EPSPs involves adaptation to Ca^{2+}. Adaptation would cause a sustained rise in $[Ca^{2+}]_i$ to lose its effectiveness in evoking exocytosis, just as adaptation in sensory transduction systems decreases the response to a sustained stimulus (Eatock et al., 1987; Kurahashi and Shibuya, 1990; Bownds and Arshavsky, 1995). A diagnostic feature that

distinguishes adaptation from desensitization is the production of a new transient response with each successive increment in stimulus strength. Thus, the series of EPSPs in response to a staircase-like series of increases in $[Ca^{2+}]_i$ (Figure 4) is highly characteristic of adaptation. The synchronization of exocytosis with each increase in $[Ca^{2+}]_i$ suggests that the triggering mechanism senses the rate of change of $[Ca^{2+}]_i$. Since a sensitivity to the rate of change rather than the absolute level of the stimulus is a hallmark of adaptation, we tested the hypothesis that exocytosis adapts to Ca^{2+} by examining how responses varied with the speed of a presynaptic $[Ca^{2+}]_i$ rise.

As noted above, EPSPs could be evoked by the relatively slow rises in $[Ca^{2+}]_i$ produced by continuous illumination with an arc lamp (Figure 3C). These EPSPs had an amplitude of only 3.6 $\pm$ 0.7 mV (12 synapses with mean exposure time of 30 $\pm$ 2 ms), compared with an amplitude of 7.0 $\pm$ 0.8 mV (10 synapses; $p = 0.002$) for EPSPs evoked by 20-fold faster $[Ca^{2+}]_i$ rises produced by discharges from a flash lamp. This was in spite of the fact that the flash lamp produced somewhat smaller $[Ca^{2+}]_i$ rises of 28 $\pm$ 6 μM, compared with 42 $\pm$ 7 μM produced by illumination from the arc lamp ($p = 0.07$). Thus, the smaller EPSPs observed when photolysis was slower cannot be accounted for by differences in final $[Ca^{2+}]_i$, and therefore can be attributed to the slower rate of rise of $[Ca^{2+}]_i$.

The relevance of the rate of change of $[Ca^{2+}]_i$ to transmitter release could also be seen when steady illumination was maintained for longer times and then suddenly stopped. EPSPs peaked after about 50 ms of illumination, and then began a slow decline (Figure 7A). When illumination was terminated (by closing the shutter), the EPSP showed a sudden downward deflection. At that instant in time, $[Ca^{2+}]_i$ must have stopped increasing. Thus, the downward deflection means that a decrease in the rate of rise of $[Ca^{2+}]_i$ precipitated a reduction in the rate of exocytosis (Figure 7A).

Finally, we reduced the rate of rise of $[Ca^{2+}]_i$ by inserting a 0.5 neutral density filter in the light path, thereby reducing the rate of photolysis 3.1-fold. The illumination period was extended proportionally to give $[Ca^{2+}]_i$ rises differing only in steepness but not in magnitude (the ratio of final $[Ca^{2+}]_i$ for long pulses-to-short pulses was 1.01 $\pm$ 0.03 for 12 synapses). This reduction in the rate of rise of $[Ca^{2+}]_i$ reduced the EPSP amplitude by 35% $\pm$ 5% (12 synapses; Figure 7B). Thus, the results of four different experimental paradigms (including Figure 4) all support the conclusion that the rate of exocytosis is influenced by the rate of change of $[Ca^{2+}]_i$.

Discussion

These experiments showed that neurotransmitter release elicited by caged Ca^{2+} in the squid giant synapse is transient in nature. The rapid decay of release provides evidence for a novel process that limits secretion at synapses. The decline in synaptic transmission was shown to occur at a site downstream from the Ca^{2+} rise and upstream from postsynaptic receptor activation. Since vesicle depletion was ruled out, we concluded that the intrinsic rate of fusion of synaptic vesicles with the plasma membrane declines with time in the continued presence of high $[Ca^{2+}]_i$. These findings together with the observation that exocytosis is sensitive to the rate of change of $[Ca^{2+}]_i$ suggest that a likely cause for the decay of EPSPs is adaptation of Ca^{2+}-triggered exocytosis. Adaptation has been described in many sensory systems (Eatock et al., 1987; Kurahashi and Shibuya, 1990; Bownds and Arshavsky, 1995) as well as in the regulation of cytoplasmic Ca^{2+} (Meyer and Stryer, 1990; Györke and Fill, 1993; Valdivia et al., 1995). Work on the ryanodine receptor (Györke and Fill, 1993; Valdivia et al., 1995) demonstrated adaptation in the context of excitation–contraction coupling. Our findings in excitation–secretion coupling thus establish an interesting parallel with excitation–contraction coupling by showing adaptation in two very rapid Ca^{2+}-mediated signaling systems.

Relevance to Previous Work on Exocytosis

In general, the rate of secretion differs dramatically depending on whether Ca^{2+} is introduced by cell permeabilization, K^+ depolarization, voltage steps, or caged Ca^{2+}. For example, rapid Ca^{2+} entry through Ca^{2+} channels produces much more exocytosis than slow Ca^{2+} dialysis (Augustine and Neher, 1992; von Gersdorff and Matthews, 1994). Since $[Ca^{2+}]_i$ changes at different rates with these various protocols, adaptation may underlie many of these discrepancies. Sustained rises in $[Ca^{2+}]_i$ trigger transient secretion in nerve terminals and endocrine cells (Neher and Zucker, 1993; Thomas et al., 1993; Heidelberger et al., 1994; Heinemann et al., 1994). A second increase in $[Ca^{2+}]$ produced additional secretion in permeabilized chromaffin cells (Knight and Baker, 1982), sea urchin eggs (Kaplan et al., 1994, Biophys. Soc., abstract), and isolated peptidergic nerve terminals (Stuenkel and Nordmann, 1993), reminiscent of the result shown in Figure 4. A constant influx of Ca^{2+} causes secretion to peak rapidly and then to decline with a time course similar to that observed here (Llinas et al., 1981; von Gersdorff and Matthews, 1994). While these results have been interpreted previously in terms of emptying pools of primed vesicles, the fact that many docked secretory granules are not rapidly released (Parsons et al., 1995) is consistent with our conclusion that adaptation limits exocytosis during a sustained rise in $[Ca^{2+}]_i$.

The Role of Adaptation in Synaptic Transmission

Because facilitation (Katz and Miledi, 1968; Charlton et al., 1982) and presynaptic $[Ca^{2+}]_i$ (Llinas and Nicholson, 1975; Charlton et al., 1982; Augustine et al., 1985; Swandulla et al., 1991; Smith et al., 1993) decay much more slowly than neurotransmitter release, the termination of release during synaptic transmission is difficult to explain in terms of Ca^{2+} removal. To bridge this gap, it has been proposed that domains of high $[Ca^{2+}]$ form around Ca^{2+} channels to trigger release (Fogelson and Zucker, 1985; Simon and Llinas, 1985; Parnas et al., 1989; Adler et al., 1991; Schweizer et al., 1995). The time course of transmitter release can then follow the rapid formation and collapse of these domains. Adaptation also could contribute to the termination of transmitter release during synaptic transmission, although at the

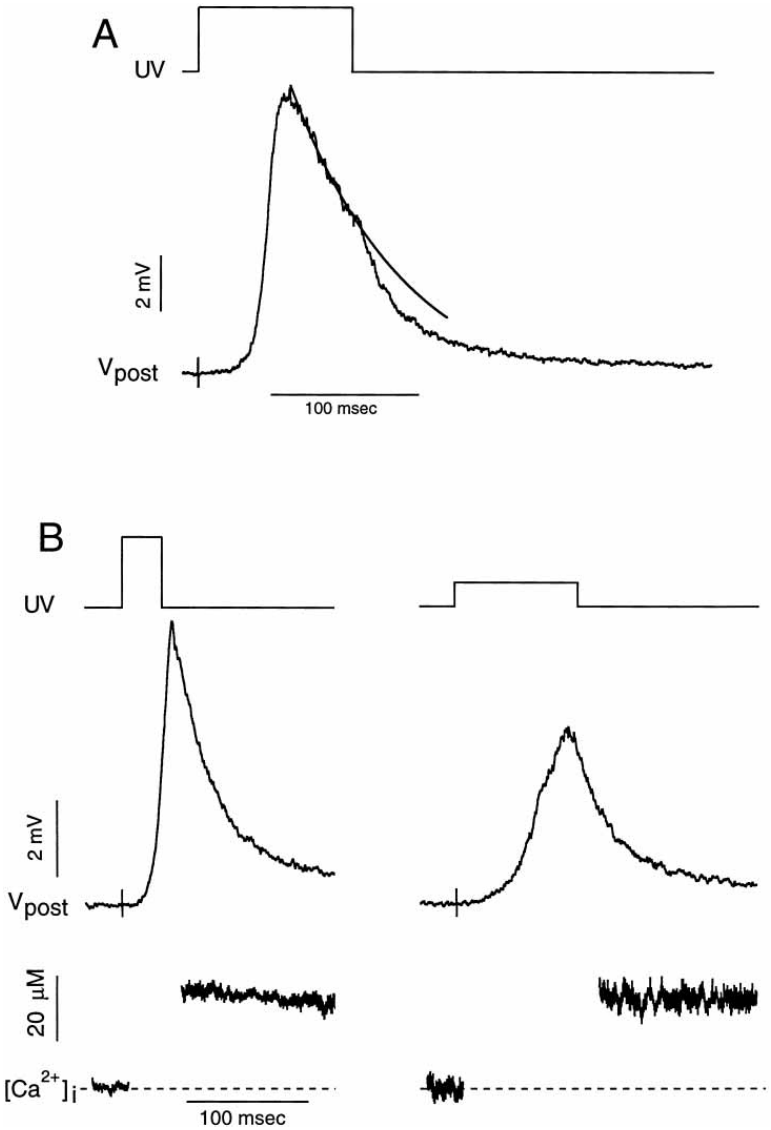

Figure 7. The Role of the Rate of Rise of $[Ca^{2+}]_i$

(A) An EPSP was evoked by photolysis of NPE with a 100 ms period of steady arc lamp illumination (indicated schematically above). The EPSP peaked while the shutter was open and then decayed slowly. Shortly after the peak, the shutter closed and the rate of decay of the EPSP accelerated markedly. A solid line extends an exponential function beyond the time of shutter closing to highlight the change in slope. The drop in exocytosis when the shutter closed indicates that secretion is sensitive to the rate of change of $[Ca^{2+}]_i$.

(B) Slowing the rate of increase of $[Ca^{2+}]_i$ reduced the amplitude and the rate of rise of the EPSP. Photolysis of NPE with steady illumination from an arc lamp for 30 ms (left) increased $[Ca^{2+}]_i$ and elicited an EPSP. The illumination was then reduced by a factor of 3.1 with a 0.5 neutral density filter and the shutter was left open for 100 ms (right) to produce a similar increase in $[Ca^{2+}]_i$. With longer periods of weaker illumination, the peak EPSP amplitude was reduced by 35%, indicating that exocytosis is influenced by the speed of the $[Ca^{2+}]_i$ rise.

squid synapse adaptation is roughly one order of magnitude too slow. However, Ca^{2+} domains may be less relevant to the secretion of some neurotransmitters (Verhage et al., 1991), allowing adaptation to play a role in the termination of release at these synapses. By confining secretion to the time of the presynaptic action potential, adaptation offers an alternative to the Ca^{2+} domain hypothesis as an explanation for the general finding that the kinetics of transmitter release from nerve terminals is insensitive to alterations in Ca^{2+} entry (Barrett and Stevens, 1972; Diamond and Jahr, 1995).

Adaptation provides a means by which nerve terminals can filter out slow changes in $[Ca^{2+}]_i$ while remaining sensitive to the fast changes produced by influx through Ca^{2+} channels. The fact that rapid changes in $[Ca^{2+}]_i$ are more effective than slow changes makes the presynaptic action potential an ideal physiological stimulus for secretion, and faster rises together with higher $[Ca^{2+}]_i$ in domains around active zones may contribute to the steeper onset of EPSPs evoked by presynaptic action potentials (Figure 1C). Adaptation increases the importance of proximity between Ca^{2+} channels and release sites and may contribute to the selectivity of different modes of Ca^{2+} entry in triggering exocytosis of different populations of vesicles (Verhage et al., 1991). Adaptation can prevent both the depletion of vesicles and the desensitization of postsynaptic receptors even as presynaptic $[Ca^{2+}]_i$ builds up. This would delay the onset of synaptic depression and allow nerve terminals to secrete repetitively when driven at high frequencies. Adaptation can thus play a role in information processing within nerve terminals, and alterations in the molecular machinery responsible for adaptation could then alter synaptic transmission in a selected range of frequencies to foster novel forms of synaptic plasticity.

Adaptation and the Molecular Mechanism of Transduction

A molecular mechanism that explains how Ca^{2+} triggers exocytosis must also account for adaptation. Kinetic

models that can simulate adaptation may help relate this phenomenon to the molecular mechanisms of transmitter release. To illustrate how such an analysis can be instructive, we consider two models in which transduction is assumed to have no requirement for chemical energy (e.g., ATP hydrolysis; see Martin, 1994, and Parsons et al., 1995). Thus, each step is reversible, so that the requirement of detailed balance is satisfied. The following two schemes satisfy these requirements (Knox et al., 1986; Cheng et al., 1995).

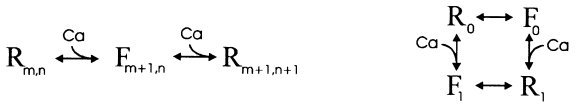

In these models, Ca^{2+} receptors interconvert between a state that is ready to bind Ca^{2+} but not able to induce fusion, termed R, and a fusogenic state, termed F. In model (a), the receptor is a multimeric complex (Cheng et al., 1995), each subunit of which contains two distinct classes of Ca^{2+}-binding sites. These two types of Ca^{2+}-binding sites exert opposite actions; occupation of the first site (occupancy number denoted by the first subscript) favors conversion to the F state, and occupation of the second site (the second subscript) favors conversion to the R state. Model (a) predicts faster and less complete adaptation of exocytosis at higher [Ca^{2+}] (Cheng et al., 1995), neither of which were indicated by our results. However, if model (a) can be modified to provide better agreement with experimental results, it could provide a new function for Ca^{2+}-binding proteins in nerve terminals. Microinjection into nerve terminals of rabphilin3A, a high affinity Ca^{2+}-binding protein of synaptic vesicles, reduces transmitter release (Burns et al., 1995, Soc. Neurosci., abstract), thus providing the inhibitory step proposed in model (a).

In model (b), a receptor has only one Ca^{2+}-binding site, but the Ca^{2+} affinity changes as the receptor interconverts between two conformations (Knox et al., 1986). In equilibrium with any [Ca^{2+}], most of the receptor is either in state R_0 or R_1. Elevating [Ca^{2+}] shifts receptor from R_0 to R_1 through F_1, and while this is occurring, receptor transiently in F_1 causes fusion. With appropriate choices of parameters, model (b) can produce complete adaptation at all levels of [Ca^{2+}], as well as decay rates that are independent of [Ca^{2+}]. The predictions of model (b) are therefore closer to our observations and lead to the novel suggestion that the Ca^{2+} receptor for exocytosis can alter its affinity. In this context, the Ca^{2+} binding properties of synaptotagmin, a putative Ca^{2+} receptor for exocytosis (Jahn and Südhof, 1994; Schweizer et al., 1995), take on a new significance. For example, the Ca^{2+} affinity of synaptotagmin is sensitive to phospholipids (Brose et al., 1992) and syntaxin (Chapman et al., 1995), and this may allow synaptotagmin to undergo affinity transitions as in model (b). Future analysis of exocytosis in terms of these models should provide valuable insights into the underlying molecular mechanisms. Regardless of which models prove to be most useful in the long run, the requirement of adaptation, together with the well established cooperative action of Ca^{2+} (Dodge and Rahamimoff, 1967; Knight and Baker, 1982; Augustine and Charlton, 1986; Heidelberger et al., 1994), constitute a powerful set of constraints on the Ca^{2+}-sensing system of exocytosis.

Experimental Procedures

Electrophysiology

Microelectrodes were inserted into the pre- and postsynaptic elements of the squid giant synapse (Adler et al., 1991). Postsynaptic potentials were recorded under current clamp with an EPC-7 amplifier and acquired with a Macintosh computer equipped with an ITC-16 interface (Instrutech, Great Neck, NY). Data acquisition and digital output were controlled by the Pulse Control extension (Herrington and Bookman, 1994) of the computer program IGOR (Wavemetrics, Lake Oswego, OR). Presynaptic potential was recorded with a model M-707 amplifier (World Precision Instruments, Sarasota, FL). Temperature was maintained in a 0.5°C range that varied from 13°C to 18°C between experiments. During experiments, the preparation was superfused with artificial sea water consisting of 466 mM NaCl, 54 mM $MgCl_2$, 11 mM $CaCl_2$, 10 mM KCl, 3 mM $NaHCO_3$, 50 HEPES (pH 7.2), aerated with 99.5% O_2, 0.5% CO_2. The presynaptic electrode contained 100 mM KCl, 250 mM K-isethionate, 100 mM taurine, and 50 mM HEPES (pH 7.4), with additional reagents as indicated below. The postsynaptic electrode contained 3 M KCl. Electrical stimulation was applied either extracellularly, to the mantle connective entering the ganglion, or intracellularly through the presynaptic electrode. When the nerve terminal was stimulated by current injection all-or-none behavior was verified by varying stimulus strength.

Photolysis of NPE

NPE (Molecular Probes, Eugene, OR) (Ellis-Davies and Kaplan, 1994) was loaded into the nerve terminal by including 20 mM in the solution filling the presynaptic electrode. This solution was pressure injected into the presynaptic terminal over a period of at least 15 min with pulses of compressed nitrogen from a Picospritzer (General Valve Corporation, Fairfield, NJ). Measurements with injected fluorescein–dextran indicated that the injection solution was diluted 10- to 100-fold, so we estimate the final concentration of NPE in the nerve terminal to be approximately 0.2–2 mM. The degree of Ca^{2+} loading of NPE in the pipette solution varied from 50% to 67%; variations within this range produced no discernible difference, probably because there was sufficient time for equilibration of NPE with endogenous intracellular Ca^{2+}.

In most experiments, photolysis was performed with either a flash lamp (Chadwick-Helmuth, El Monte, CA) or a continuous 75 W Xe arc lamp. In one set of experiments, a 100 W Hg arc lamp was used with a power supply that had been modified to allow computer modulation of the output (Optiquip, Highland Mills, NY). This system was used to produce 1 ms surges approximately 10-fold higher than the output of the bulb operating at its rated power.

Light from these sources was first reflected off a 400 nm dichroic mirror to select UV light. This mirror combined the photolysis beam with transmitted light (>400 nm) from another light source used to monitor furaptra fluorescence (described below). Within the epifluorescence unit of the microscope, the two beams were reflected by a 475 nm dichroic mirror (reflecting shorter wavelengths). Both mirrors were treated for enhanced UV light reflectance (Chroma Technology, Brattleboro, VT). Light was focused onto the preparation with a 40× Olympus UPlanApo water-immersion objective (N.A. 0.75). A few experiments were also performed with a 10× Olympus UPlanApo objective (N.A. 0.40) to illuminate greater areas. Unless noted otherwise, all flash discharges were of maximum intensity (220 V). The flash lamp discharge was 75% complete within 1.5 ms, as determined by measurement with a photomultiplier tube (PMT). Illumination from the 75 W Xe arc lamp was controlled by an electronic shutter (Vincent Associates, Rochester, NY) under computer control. Measurements with a PMT indicated that the energy of a flash lamp discharge was equivalent to a 30 ms period of illumination by the continuous Xe arc lamp. The fraction of a synapse illuminated varied from 33% to 100%, but when illumination of the entire synapse was not possible, we focused on the distal portion where active zones are most highly concentrated (Pumplin et al., 1981; Smith et al.,

1993). The timing between light exposure and electrical stimulation was controlled by the computer.

$[Ca^{2+}]$ Measurement

For measurement of $[Ca^{2+}]_i$, we used the Ca^{2+}-sensitive fluorescent dye furaptra (Molecular Probes) (Raju et al., 1989; Konishi et al., 1991), including 2 mM in the presynaptic electrode solution. In most experiments, furaptra was excited by light from a 50 W Hg arc lamp that was passed first through a 1.0 neutral density filter and then through a 420 ± 20 nm bandpass filter (Omega Optical, Brattleboro VT). The light was then joined with the photolysis light by passage through the 400 nm dichroic mirror mentioned above, after which the excitation light followed the same path as the photolysis light to the 475 nm dichroic mirror and microscope objective, also mentioned above. Emitted light was collected by the microscope objective, passed through the 475 nm dichroic mirror and a 510 ± 20 bandpass filter, recorded with a PMT, and read into the computer. A computer-controlled shutter protected the PMT during photolysis. In experiments using the modulated 100 W Hg arc lamp described above for photolysis, furaptra was excited with low intensity light from the same source following the same path. The bandwidth of this light was set at 400 nm above by the first dichroic mirror and at approximately 350 nm below by the microscope objective.

Ca^{2+} concentration can be estimated from fluorescence, F, by methods similar to those of Khodakhah and Ogden (1995). We used the expression

$$[Ca^{2+}] = K_d(F_{min} - F)/(F - F_{max}) \quad (2)$$

which contains three calibration parameters, F_{min}, the fluorescence when all the dye is free, F_{max}, the fluorescence when all the dye is bound, and K_d, the dissociation constant of the dye. Because resting $[Ca^{2+}]_i$ (Swandulla et al., 1991) is approximately 1000-fold lower than the K_d of furaptra (values below), the dye is virtually all Ca^{2+} free before stimulation. This makes the initial fluorescence reading a good estimate of F_{min}. From fluorescence measurements with 50 μm diameter quartz capillary tubes containing 450 mM KCl, 50 mM HEPES (pH 7.4), 0 mM or 4 mM $MgCl_2$, 0 mM or 25 mM $CaCl_2$, and 0.35 mM or 1.3 mM furaptra, we found that $F_{min}/F_{max} = 600$ with an excitation bandwidth of 400–440 nm, and 1.81 with an excitation bandwidth of 350–400 nm. This confirms the observation of Konishi et al. (1991) that with excitation above 400 nm, furaptra fluorescence is almost completely quenched by Ca^{2+} and justifies setting F_{max} equal to zero for long wavelength excitation. The ratio of 1.81 was used to calculate F_{max} from F_{min} for short wavelength excitation.

To estimate K_d, we used fluorescence measurements from solutions containing 0.5 mM $CaCl_2$ and 0.35 mM furaptra together with measurements of F_{min} and F_{max} for 0.35 mM furaptra and adjusted K_d to fit the fluorescence measurements. We thus obtained K_d = 110 μM and 198 μM, for 0 mM and 4 mM Mg^{2+}, respectively. The 0 mM Mg^{2+} value is approximately twice that determined in Ringer solution with a lower ionic strength (Konishi et al., 1991). The dependence on Mg^{2+} is consistent with the Mg^{2+} binding properties of this dye (Raju et al., 1989). The K_d value in 4 mM Mg^{2+} was used for calculating $[Ca^{2+}]_i$ in most experiments. The 0 mM Mg^{2+} value was used in experiments with HEDTA (Figure 3C) because this compound binds Mg^{2+}.

Acknowledgments

We are indebted to Kamran Khodakhah for many helpful suggestions. He, Larry Katz, and Joe Corless are thanked for the loan of lamps, and Beth Finch, Sam Wang, Jeff Walker, and Hector Valdivia for advice in working with NPE. We thank Felix Schweizer for the idea of adaptation, and William DeBello, Marie Burns, and Tom Martin for helpful discussions. The research was supported by a fellowship from the Wisconsin chapter of the American Heart Association to S. F. H. and National Institutes of Health grants NS21624 to G. J. A. and NS30016 to M. B. J.

The costs of publication of this article were defrayed in part by the payment of page charges. This article must therefore be hereby marked *"advertisement"* in accordance with 18 USC Section 1734 solely to indicate this fact.

Received April 24, 1996; revised July 11, 1996.

References

Adler, E.M., Augustine, G.J., Duffy, S.N., and Charlton, M.P. (1991). Alien intracellular calcium chelators attenuate neurotransmitter release at the squid giant synapse. J. Neurosci. *11*, 1496–1507.

Augustine, G.J., and Charlton, M.P. (1986). Calcium dependence of presynaptic calcium current and post-synaptic response at the squid giant synapse. J. Physiol. *381*, 619–640.

Augustine, G.J., and Eckert, R. (1984). Divalent cations differentially support transmitter release at the squid giant synapse. J. Physiol. *346*, 257–271.

Augustine, G.J., and Neher, E. (1992). Calcium requirements for secretion in bovine chromaffin cells. J. Physiol. *450*, 247–271.

Augustine, G.J., Charlton, M.P., and Smith, S.J. (1985). Calcium entry into voltage-clamped presynaptic terminals of squid. J. Physiol. *367*, 143–162.

Barrett, E.F., and Stevens, C.F. (1972). The kinetics of transmitter release at the frog neuromuscular junction. J. Physiol. *227*, 691–708.

Bownds, M.D., and Arshavsky, V.Y. (1995). What are the mechanisms of photoreceptor adaptation? Behav. Brain Sci. *18*, 415–424.

Brose, N., Petrenko, A.G., Südhof, T.C., and Jahn, R. (1992). Synaptotagmin: a calcium sensor on the synaptic vesicle surface. Nature *256*, 1021–1025.

Chapman, E.R., Hanson, P.I., An, S., and Jahn, R. (1995). Ca^{2+} regulates the interaction between synaptotagmin and syntaxin 1. J. Biol. Chem. *270*, 23667–23671.

Charlton, M.P., Smith, S.J., and Zucker, R.S. (1982). Role of presynaptic calcium ions in synaptic facilitation and depression at the squid giant synapse. J. Physiol. *323*, 173–193.

Cheng, H., Fill, M., Valdivia, H., and Lederer, W.J. (1995). Models of Ca^{2+} release channel adaptation. Science *267*, 2009–2010.

Corrie, J.E., DeSantis, A., Katayama, Y., Khodakhah, K., Messenger, J.B., Ogden, D.C., and Trentham, D.R. (1993). Postsynaptic activation at the squid giant synapse by photolytic release of L-glutamate from a "caged" L-glutamate. J. Physiol. *465*, 1–8.

Delaney, K.R., and Zucker, R.S. (1990). Calcium released by photolysis of DM-nitrophen stimulates transmitter release at squid giant synapse. J. Physiol. *426*, 473–498.

Diamond, J.S., and Jahr, C.E. (1995). Asynchronous release of synaptic vesicles determines the time course of the AMPA receptor-mediated EPSC. Neuron *15*, 1097–1107.

Dodge, F.A., and Rahamimoff, R. (1967). Cooperative action of calcium ions in transmitter release at the neuromuscular junction. J. Physiol. *193*, 419–432.

Eatock, R.A., Corey, D.P., and Hudspeth, A.J. (1987). Adaptation of mechanoelectrical transduction in hair cells of the bullfrog's sacculus. J. Neurosci. *7*, 2821–2836.

Ellis-Davies, G.C.R., and Kaplan, J.H. (1994). Nitrophenyl-EGTA, a photolabile chelator that selectively binds Ca^{2+} with high affinity and releases rapidly upon hydrolysis. Proc. Natl. Acad. Sci. USA *91*, 187–191.

Ellis-Davies, G.C.R., Kaplan, J.H., and Barsotti, R.J. (1996). Laser photolysis of caged calcium: rates of calcium release by nitrophenyl-EGTA and DM-nitrophen. Biophys. J. *70*, 1006–1016.

Fogelson, A.L., and Zucker, R.S. (1985). Presynaptic calcium diffusion from various arrays of single channels. Biophys. J. *48*, 1003–1017.

Györke, S., and Fill, M. (1993). Ryanodine receptor adaptation: control mechanism of Ca^{2+}-induced Ca^{2+} release in heart. Science *260*, 807–809.

Heidelberger, R., Heinemann, C., Neher, E., and Matthews, G. (1994). Calcium dependence of the rate of exocytosis in a synaptic terminal. Nature *371*, 513–515.

Heinemann, C., Chow, R.H., Neher, E., and Zucker, R.S. (1994).

Kinetics of the secretory response in bovine chromaffin cells following flash photolysis of caged Ca^{2+}. Biophys. J. *67*, 2546–2557.

Herrington, J., and Bookman, R.J. (1994). Pulse Control Version 4.3: Igor XOPS for Patch Clamp Data Acquisition (Miami, Florida: University of Miami Press).

Hodgkin, A.L. (1964). The Conduction of the Nervous Impulse (Springfield, Illinois: Thomas).

Jahn, R., and Südhof, T.C. (1994). Synaptic vesicles and exocytosis. Annu. Rev. Neurosci. *17*, 219–246.

Katz, B. (1969). The Release of Neural Transmitter Substances (Liverpool: Liverpool University Press).

Katz, B., and Miledi, R. (1968). The role of calcium in neuromuscular facilitation. J. Physiol. *195*, 481–492.

Kelly, J.S., and Gage, P.W. (1969). L-glutamate blockage of transmission at the giant synapse of the squid stellate ganglion. J. Neurbiol. *2*, 209–219.

Khodakhah, K., and Ogden, D. (1995). Fast activation and inactivation of inositol triphosphate-evoked Ca^{2+} release in rat cerebellar Purkinje neurones. J. Physiol. *487*, 343–358.

Knight, D.E., and Baker, P.F. (1982). Calcium-dependence of catecholamine release from bovine adrenal medullary cells after exposure to intense electric fields. J. Membr. Biol. *68*, 107–140.

Knox, B.E., Devreotes, P.N., Goldbeter, A., and Segal, L.A. (1986). A molecular mechanism for sensory adaptation based on ligand-induced receptor modification. Proc. Natl. Acad. Sci. USA *83*, 2345–2349.

Konishi, M., Hollingworth, S., Harkins, A.B., and Baylor, S. (1991). Myoplasmic Ca transients in intact skeletal muscle fibers momintored with the fluorescence indicator furaptra. J. Gen. Physiol. *97*, 271–301.

Kurahashi, T., and Shibuya, T. (1990). Ca2(+)-dependent adaptive properties in the solitary olfactory receptor cell of the newt. Brain Res. *515*, 261–268.

Kusano, K., and Landau, E.M. (1975). Depression and recovery of transmission at the squid giant synapse. J. Physiol. *245*, 13–22.

Llinas, R., and Nicholson, C. (1975). Calcium role in depolarization-secretion coupling: an aequorin study in squid giant synapse. Proc. Natl. Acad. Sci. USA *72*, 187–190.

Llinas, R., Steinberg, I.Z., and Walton, K. (1981). Relationship between presynaptic calcium current and postsynaptic potential in squid giant synapse. Biophys. J. *33*, 323–352.

Llinas, R., Sugimori, M., and Simon, S.M. (1982). Transmission by presynaptic spike-like depolarization in the squid synapse. Proc. Natl. Acad. Sci. USA *79*, 2415–2419.

Martin, T.F.J. (1994). The molecular machinery for fast and slow neurosecretion. Curr. Opin. Neurobiol. *4*, 626–632.

Meyer, T., and Stryer, L. (1990). Transient calcium release induced by successive increments of inositol 1,4,5-triphosphate. Proc. Natl. Acad. Sci. USA *87*, 3841–3845.

Moore, W.J. (1972). Physical Chemistry (Englewood Cliffs, New Jersey: Prentice-Hall, Incorporated).

Neher, E., and Augustine, G.J. (1992). Calcium gradients and buffers in bovine chromaffin cells. J. Physiol. *450*, 273–301.

Neher, E., and Zucker, R.S. (1993). Multiple calcium-dependent processes related to secretion in bovine chromaffin cells. Neuron *10*, 21–30.

Parnas, H., Hovav, G., and Parnas, I. (1989). Effect of Ca^{2+} diffusion on the time course of neurotransmitter release. Biophys. J. *55*, 859–874.

Parsons, T.D., Coorssen, J.R., Horstmann, H., and Almers, W. (1995). Docked granules, the exocytotic burst, and the need for ATP hydrolysis in endocrine cells. Neuron *15*, 1085–1096.

Pumplin, D.W., Reese, T.S., and Llinas, R. (1981). Are the presynaptic membrane particles the calcium channels? Proc. Natl. Acad. Sci. USA *78*, 7210–7213.

Raju, B., Murphy, E., Levy, L.A., Hall, R.D., and London, R.E. (1989). A fluorescent indicator for measuring cytosolic free magnesium. Am. J. Physiol. *256*, C540–C548.

Scheller, R.H. (1995). Membrane trafficking in the presynaptic terminal. Neuron *14*, 893–897.

Schweizer, F.E., Betz, H., and Augustine, G.J. (1995). From vesicle docking to endocytosis: intermediate reactions of exocytosis. Neuron *14*, 689–696.

Simon, S.M., and Llinas, R. (1985). Compartmentalization of the submembrane calcium activity during calcium influx and its significance in transmitter release. Biophys. J. *48*, 485–498.

Smith, S.J., Buchanan, J., Osses, L.R., Charlton, M.P., and Augustine, G.J. (1993). The spatial distribution of calcium signals in squid presynaptic terminals. J. Physiol. *472*, 573–593.

Stuenkel, E.L., and Nordmann, J.J. (1993). Intracellular calcium and vasopressin release of rat isolated neurohypophysial nerve endings. J. Physiol. *468*, 335–355.

Swandulla, D., Hans, M., Zipser, K., and Augustine, G.J. (1991). Role of residual calcium in synaptic depression and posttetanic potentiation: fast and slow calcium signaling in nerve terminals. Neuron *7*, 915–926.

Thomas, P., Wong, J.G., and Almers, W. (1993). Millisecond studies of secretion in single rat pituitary cells stimulated by flash photolysis of caged Ca^{2+}. EMBO J. *12*, 303–306.

Valdivia, H.H., Kaplan, J.H., Ellis-Davies, G.C.R., and Lederer, W.J. (1995). Rapid adaptation of cardiac ryanodine receptors: modulation by Mg^{2+} and phosphorylation. Science *267*, 1997–2000.

Verhage, M., McMahon, H.T., Ghijsen, W.E.J.M., Boomsma, F., Scholten, G., Wiegant, V.M., and Nicholls, D.G. (1991). Differential release of amino acids, neuropeptides, and catecholamines from isolated nerve terminals. Neuron *6*, 517–524.

von Gersdorff, H., and Matthews, G. (1994). Dynamics of synaptic vesicle fusion and membrane retrieval in synaptic terminals. Nature *367*, 735–739.

Zucker, R.S. (1993). The calcium concentration clamp: Spikes and reversible pulses using the photolabile chelator DM-nitrophen. Cell Calcium *14*, 87–100.